UC Irvine
Faculty Publications

Title
Contrasting controls on wildland fires in Southern California during periods with and without Santa Ana winds

Permalink
https://escholarship.org/uc/item/00x470c8

Journal
Journal of Geophysical Research: Biogeosciences, 119(3)

ISSN
21698953

Authors
Jin, Yufang
Randerson, James T
Faivre, Nicolas
et al.

Publication Date
2014-03-01

DOI
10.1002/2013JG002541

Copyright Information
This work is made available under the terms of a Creative Commons Attribution License, availalbe at https://creativecommons.org/licenses/by/4.0/

Peer reviewed

eScholarship.org Powered by the California Digital Library
University of California

AGU PUBLICATIONS

JGR

Journal of Geophysical Research: Biogeosciences

RESEARCH ARTICLE
10.1002/2013JG002541

Key Points:
- We developed separate fire-climate models for Santa Ana and non-Santa Ana fires
- Meteorology explained more temporal variability in Santa Ana fires
- The relative importance of drivers is different for two contrasting fire types

Supporting Information:
- Readme
- Figures S1–S10

Correspondence to:
Y. Jin,
yufang@uci.edu

Citation:
Jin, Y., J. T. Randerson, N. Faivre, S. Capps, A. Hall, and M. L. Goulden (2014), Contrasting controls on wildland fires in Southern California during periods with and without Santa Ana winds, *J. Geophys. Res. Biogeosci.*, *119*, 432–450, doi:10.1002/2013JG002541.

Received 21 OCT 2013
Accepted 22 FEB 2014
Accepted article online 4 MAR 2014
Published online 28 MAR 2014

Contrasting controls on wildland fires in Southern California during periods with and without Santa Ana winds

Yufang Jin[1], James T. Randerson[1], Nicolas Faivre[1], Scott Capps[2], Alex Hall[2], and Michael L. Goulden[1]

[1]Department of Earth System Science, University of California, Irvine, California, USA, [2]Department of Atmospheric and Oceanic Sciences, University of California, Los Angeles, California, USA

Abstract Wildland fires in Southern California can be divided into two categories: fall fires, which are typically driven by strong offshore Santa Ana winds, and summer fires, which occur with comparatively weak onshore winds and hot and dry weather. Both types of fire contribute significantly to annual burned area and economic loss. An improved understanding of the relationship between Southern California's meteorology and fire is needed to improve predictions of how fire will change in the future and to anticipate management needs. We used output from a regional climate model constrained by reanalysis observations to identify Santa Ana events and partition fires into those occurring during periods with and without Santa Ana conditions during 1959–2009. We then developed separate empirical regression models for Santa Ana and non-Santa Ana fires to quantify the effects of meteorology on fire number and size. These models explained approximately 58% of the seasonal and interannual variation in the number of Santa Ana fires and 36% of the variation in non-Santa Ana fires. The number of Santa Ana fires increased during years when relative humidity during Santa Ana events and fall precipitation were below average, indicating that fuel moisture is a key controller of ignition. Relative humidity strongly affected Santa Ana fire size. Cumulative precipitation during the previous three winters was significantly correlated with the number of non-Santa Ana fires, presumably through increased fine fuel density and connectivity between infrastructure and nearby vegetation. Both relative humidity and the preceding wet season precipitation influenced non-Santa Ana fire size. Regression models driven by meteorology explained 57% of the temporal variation in Santa Ana burned area and 22% of the variation in non-Santa Ana burned area. The area burned by non-Santa Ana fires has increased steadily by 1.7% year^{-1} since 1959 ($p < 0.006$); the occurrence of extremely large Santa Ana fires has increased abruptly since 2003. Our results underscore the need to separately consider the fuel and meteorological controls on Santa Ana and non-Santa Ana fires when projecting climate change impacts on regional fire.

1. Introduction

Southern California's Mediterranean climate, episodic fire weather, large wildland-urban interface, and rugged terrain are conducive to large, severe, and costly wildfires [*Westerling et al.*, 2004; *Halsey*, 2005; *Keeley et al.*, 2009]. Hot and dry summers follow mild and wet growing seasons. Santa Ana (SA) winds in fall, characterized by low relative humidity (RH) and strong offshore flow, can result in intense firestorms [*Westerling et al.*, 2004; *Hughes and Hall*, 2010; *Moritz et al.*, 2010]. Plant production is moderate and varies greatly from year to year, resulting in a shrub-dominated landscape that is favorable to crown fire [*Barbour et al.*, 2007]. Housing development has created a large wildland-urban interface, increasing the probability of anthropogenic ignition [*Keeley et al.*, 2004; *Syphard et al.*, 2007; *Faivre et al.*, 2014]. The complex mountain terrain makes it difficult to predict fire spread and to access many areas for firefighting, further increasing fire size.

Many of the most devastating fires in Southern California occur during Santa Ana conditions, when strong offshore winds and low humidity lead to severe fire weather [e.g., *Keeley and Zedler*, 2009]. The 2003 Santa Ana firestorm, widely considered a hundred-year event at the time, was soon followed by the 2007 firestorm (Figure 1a) [*Keeley et al.*, 2004; *Keeley et al.*, 2009]. These fires incurred billions of dollars in cost associated with firefighting, property damage, and health effects [*Delfino et al.*, 2009]. Santa Ana events typically occur in September through April with synoptic conditions and thermodynamic forcing [*Hughes and Hall*, 2010;

©2014. American Geophysical Union. All Rights Reserved.

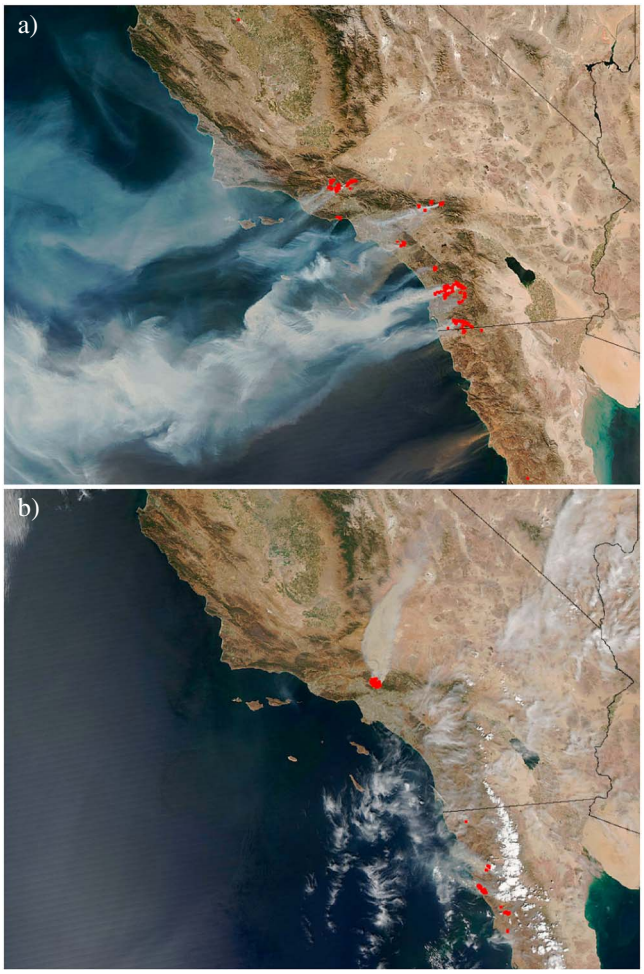

Figure 1. Fires in Southern California can be separated into those that occur during fall Santa Ana events and those that occur during the hot and dry Mediterranean summer. (a) More than 10 devastating Santa Ana fires burned concurrently throughout Southern California, including the Ranch, Buckweed, Magic, Canyon, Slide, Grass Valley, Santiago, Rice, Witch, and Harris fires, driven by sustained offshore extreme winds beginning 20 October 2007. (b) The Station fire, which started on 26 August 2009, is an example of a non-Santa Ana summer fire and is the largest in Los Angeles County's recorded history. Satellite images were acquired on 22 October 2007 (Figure 1a) and 29 August 2009 (Figure 1b) by MODIS (NASA/MODIS Rapid Response).

Abatzoglou et al., 2013]. Santa Ana winds are driven by northeastward pressure gradients and geostrophic winds that are perpendicular to Southern California's main mountain ranges; the result is terrain-intensified surface flow as offshore momentum is transferred to the surface by gravity waves. This flow drives adiabatic warming, and Santa Ana winds are often accompanied with warm temperatures and low humidity. The offshore flow may be katabaticly intensified by the thermal gradient between cold, inland deserts, and warm ocean air; the strength of the thermal gradient is a primary controller of Santa Ana intensity [*Hughes and Hall*, 2010].

While Santa Ana-driven fires receive the most attention, most wildland ignitions in Southern California actually occur during the summer and in the absence of Santa Ana conditions [*Bartlein et al.*, 2008]. These fires are comparatively easy to contain due to the prevailing onshore winds, though large summer fires have been reported, especially during years with severe drought and in remote, inaccessible terrain [*Keeley et al.*, 2009]. Over the past decade, a number of large summer fires have contributed significantly to firefighting and management costs, including the July 2007 Zaca fire (97,000 ha) and the August 2009 Station fire (65,000 ha; Figure 1b).

Fuel load, fuel connectivity, human ignition, and the occurrence of extreme weather are considered the primary drivers of Southern California's fire regime [*Minnich*, 1983; *Keeley et al.*, 1999], though the relative importance of these factors is still being debated [*Minnich*, 2001; *Keeley and Zedler*, 2009]. Recent studies have shown that the controls on fuel amount, moisture, and fuel connectivity vary with ecosystem type [*Littell et al.*, 2009] and also along productivity and precipitation gradients [*Pausas and Paula*, 2012; *van der Werf et al.*, 2008; *Krawchuk and Moritz*, 2011; *Pausas and Ribeiro*, 2013]. Temperature, especially in summer, is well correlated with fire extent and severity in the western US [*Westerling et al.*, 2006; *Spracklen et al.*, 2009], and relative humidity also regulates fuel moisture and thus fire behavior [*Viney*, 1991; *Brown et al.*, 2004; *Westerling et al.*, 2011]. Water deficit and drought associated with large-scale climate modes, such as the El Nino–Southern Oscillation and Pacific Decadal Oscillation (ENSO and PDO), are the main determinants of fire season length and severity across the western US [*Swetnam and Betancourt*, 1990; *Westerling et al.*, 2003; *Balch et al.*, 2013; *Morton et al.*, 2013]. Years with low spring precipitation account for a disproportionately large fraction of total area burned in California's Los Padres National Forest [*Davis and Michaelson*, 1995], and autumn precipitation is negatively correlated with annual fire occurrence in Southern California [*Keeley*, 2004]. But the relationship

©2014. American Geophysical Union. All Rights Reserved.

between precipitation and fire is complex; evidence also supports a positive correlation between antecedent moisture and dry season burned area in grasslands and shrublands [*Pausas*, 2004; *Littell et al.*, 2009], and increased annual burned area in Southern California has been linked with moister conditions in the preceding winter [*Keeley et al.*, 2004].

We are unaware of any systematic analysis of the relative area burned by fall Santa Ana fires versus summer non-Santa Ana fires, or of the corresponding meteorological drivers. While there is universal recognition that many of the largest and most destructive fires in Southern California occur during Santa Ana conditions [e.g., *Keeley and Zedler*, 2009], the size and total area burned has not been rigorously partitioned by fire type. Likewise, most analyses of the meteorological correlates with burned area have lumped the two types of fire. Important next steps are to separate wildland fires into these two distinct types and examine the corresponding seasonal and interannual variations, trends, and meteorological correlates. This partitioning is important for assessing the sensitivity of fire to possible changes in Santa Ana frequency and intensity with climate change [*Miller and Schlegel*, 2006; *Hughes et al.*, 2011]. Moreover, past discussion has often implicitly assumed that a single strategy for fire planning and fuel management is appropriate for all fire types in Southern California. An improved understanding of the distinct controls on the two types of fire, and the ultimate adoption of separate management strategies for areas that are prone to summer versus Santa Ana fires, may prove useful.

Our goal is to use the historical record of fire perimeters in Southern California [*California Department of Forestry and Fire Protection—The Fire and Resource Assessment Program* (*CDF-FRAP*), 2012] to develop empirical regression models that represent the seasonal and interannual variations for Santa Ana and non-Santa Ana fires. Our focus is on the monthly relationships between meteorology and fire characteristics (number, fire size, and burned area) aggregated at a regional scale. Our study extends previous work by separating the two types of fires, characterizing the frequency and intensity of Santa Ana events, examining the relative roles of individual meteorological variables, and extending the analysis to consider most of the second half of the 20th century.

2. Materials and Methods

2.1. Study Area

Our study focused on seven counties in Southern California: Santa Barbara, Ventura, Los Angeles, San Bernardino, Orange, Riverside, and San Diego (Figure 2). Southern California wildlands are topographically diverse, with strong orographic precipitation gradients. The climate supports a diversity of vegetation type: grassland and shrubland are common in the coastal plains and foothills; larger shrubs, evergreen hardwood trees, and tall conifers occur in the mountains; and smaller, sparse trees, shrubs, and grasses occur in the eastern, rain-shadowed slopes, and deserts [*Barbour et al.*, 2007]. Development is concentrated on the coastal plain and inland valleys at lower elevation. The climate is characterized by moderate, wet winters and dry summers, with marked interdecadal and interannual variation in precipitation. This variability is thought to be modulated by ENSO and the tropical intraseasonal oscillation [e.g., *Castello and Shelton*, 2004 and *Mo and Higgins*, 1998], but the link is generally weak [e.g., *Schonher and Nicholson*, 1989 and *Gershunov et al.*, 2000] and past studies have not reported a strong correlation between ENSO and fire occurrence or burned area in Southern California [*Keeley et al.*, 2004]. We therefore focused on relationships between immediate and antecedent meteorological variables and fire; we did not address broader issues such as the relationship between fire and ENSO.

2.2. Fire Perimeter Data

We used the statewide GIS layer of fire perimeters from the California Fire and Resource Assessment Program (FRAP) (version 12_1) to quantify the number of fires and area burned at monthly intervals [*CDF-FRAP*, 2012]. Fires greater than 10 acres were compiled by the California Department of Forestry and Fire Protection and other agencies since 1950. Many smaller fires were included as well. This database represents the most complete digital record of wildland fire in California and has been updated annually. We focused on fires greater than 40 ha (or 100 acres) that occurred from 1959 to 2009 (Figure 2); these fires accounted for 99% of the burned area during the period.

©2014. American Geophysical Union. All Rights Reserved.

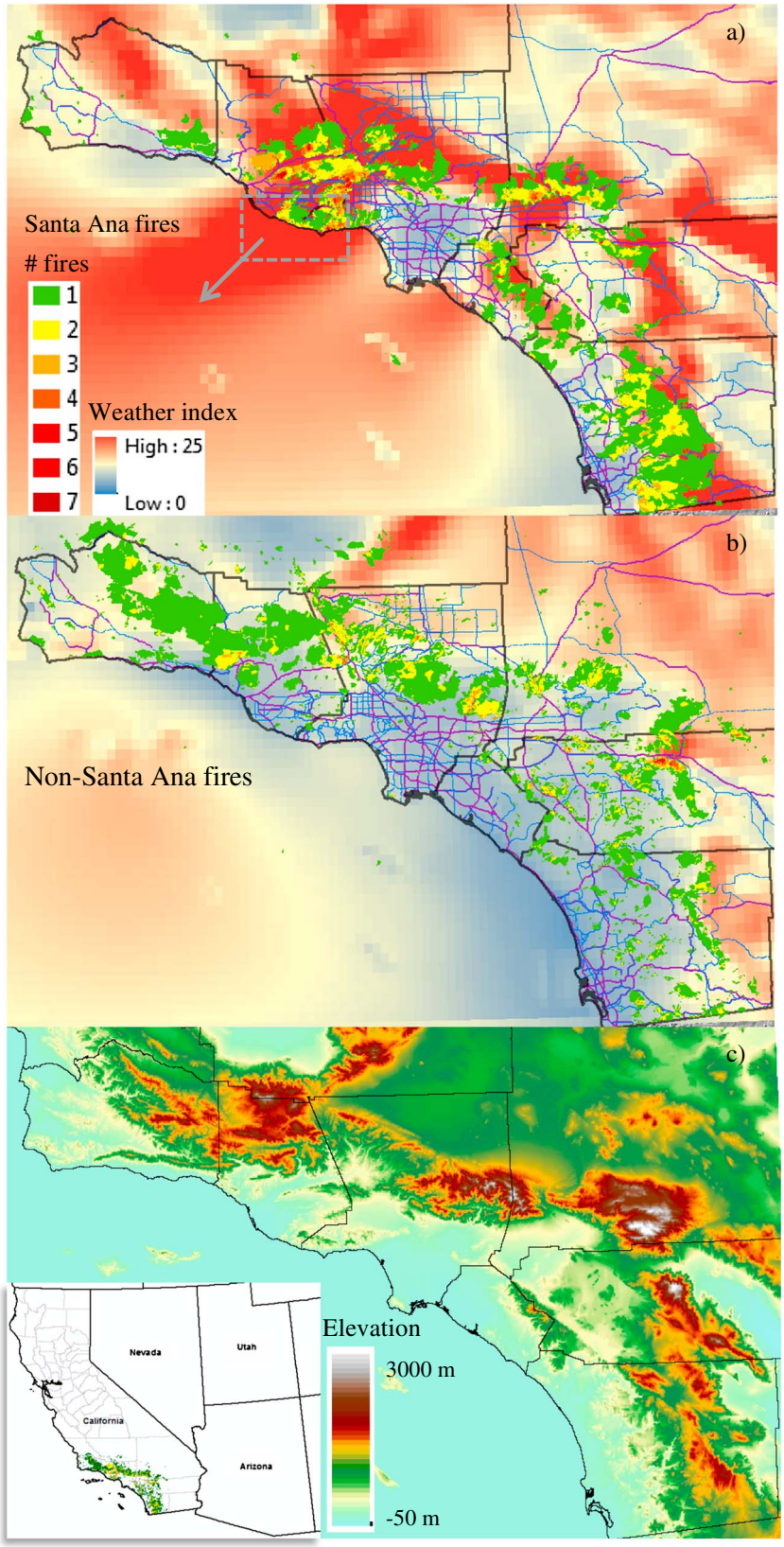

Figure 2

©2014. American Geophysical Union. All Rights Reserved.

2.3. Meteorological Records

We used monthly estimates of average daily maximum and minimum temperature, precipitation, and dew point from the Parameter-Elevation Regressions on Independent Slopes Model (PRISM) at 4 km resolution from 1959 to 2009 [*Daly et al.*, 2008]. PRISM spatially extrapolates meteorological observations from weather stations using statistical methods, a digital elevation model, additional spatial datasets, and expert interaction [*Daly et al.*, 2008]. We derived monthly mean RH from PRISM temperature and dew point. The absolute values of RH calculated this way are prone to uncertainty as a consequence of nonlinear and day-to-night averaging [*Kimball et al.*, 1997], but this is unlikely to impact our use of RH as a relative measure of atmospheric moisture demand for regression analysis. Palmer Drought Severity Index (PDSI) was obtained for California's climate region 6 from the National Climatic Data Center (ftp://ftp.ncdc.noaa.gov/pub/data/cirs/).

We mainly used a 6 km resolution climate simulation from the Penn State/National Center for Atmospheric Research mesoscale model version 5 (MM5) [*Grell et al.*, 1995] to identify Santa Ana event history and quantify the corresponding weather conditions [*Hughes and Hall*, 2010]. The 6 km resolution domain was nested within an 18 km resolution domain covering California, which in turn was nested within a 54 km resolution domain encompassing most of the western U.S. All major mountain ranges in Southern California are represented at 6 km resolution. The atmospheric boundary conditions came from the European Centre for Medium Range Weather Forecasts ERA-40 reanalysis data during 1959–2001 [*Uppala et al.*, 2005]. As a reconstruction of the local atmospheric conditions based on known large-scale atmospheric conditions, this high-resolution dynamic downscaling approach reproduces mesoscale features of atmospheric dynamics including winds with a high degree of fidelity and accurately simulates small climatic variations due to the complex topography [*Conil and Hall*, 2006; *Hughes and Hall*, 2010]. We used the North American Regional Reanalysis (NARR) data to extend the time series from January 2001 to 2009 [*Mesinger et al.*, 2006] and adjusted these data using a regression approach during overlapping periods to ensure temporal homogeneity (as described below).

We derived a time series of daily Santa Ana index based on the modeled daily mean wind speed at the exit of the largest gap through the Santa Monica mountains (Figure 2a) [*Hughes and Hall*, 2010]. A threshold of 6 m s^{-1} on the 225° (north-easterly) wind vector allowed a clear separation of Santa Ana and non-Santa Ana conditions [*Hughes and Hall*, 2010]. Adjusting this threshold by ± 2 m s^{-1} changed the fraction of total area burned during Santa Ana events by less than 5% (Figure S1). Individual Santa Ana events were identified based on the continuity of Santa Ana days. The number of Santa Ana events and length of an individual Santa Ana event were then summarized for each month. The mean wind speed and relative humidity were averaged separately during the Santa Ana and non-Santa Ana days for each month. Fire spread was calculated from wind speed [*Fosberg*, 1978].

We found a small bias between the MM5 and observation-based PRISM RH time series at a regional scale. We used linear regressions between MM5 and PRISM monthly RH during overlapping periods to remove this bias from the entire MM5 RH time series. Small biases in NARR RH from 2001 to 2009 were similarly removed. The regional RH and wind speed from NARR for Santa Ana or non-Santa Ana days correlated well with those from MM5 during overlapping periods (1979–2000) (Figure S2). We adjusted the coarser resolution NARR winds to match the MM5 winds using regressions derived during the overlapping period. We created long-term meteorological time series for the region by averaging spatially distributed datasets within areas that burned at least once during the last 60 years.

2.4. Analytical Methods

We classified burns into SA and non-SA fires based on the start date reported in the FRAP fire database and the time series of Santa Ana days (Figure 2). Fires that started during an individual Santa Ana event, or

Figure 2. Fire frequency during 1959–2009 for (a) Santa Ana fires (September–November) and (b) non-Santa Ana fires (June–September), superimposed on the Fosberg Fire Weather Index averaged during fall Santa Ana days and summer non-Santa Ana days. The daily wind speed was projected along the northeast direction (shown as grey arrow) and averaged over the grids within the dashed box in Figure 2a to calculate the Santa Ana index. (c) A topography map, with inset showing the areas that experienced fires during the past 6 decades (colored for the total number of fires). Santa Ana fires were clustered in the coastal areas and foothills downwind of mountains, and near major mountain passes, including the Tejon, Cajon, and San Gorgonio passes.

©2014. American Geophysical Union. All Rights Reserved.

within 4 days before the start date of a Santa Ana event, were classified as SA burns. We first used Spearman's rank correlation analysis (r_s) to investigate how individual concurrent and antecedent meteorological variables correlated with number of fires, average fire size, and total area burned for SA fires during September–December and for non-SA fires during May–September. The variables examined were monthly daily maximum, minimum, and mean temperature (T_{max}, T_{min}, T_{mean}), precipitation, RH, wind speed, PDSI, vapor pressure deficit, and the moisture damping factor and fire spread rate terms in Fosberg's fire weather index [*Fosberg*, 1978]. We also considered the antecedent precipitation, including previous winter (October–March), previous spring (March–May), and cumulative precipitation from the previous two or three winter seasons. Santa Ana characteristics including frequency, duration, and meteorological conditions were also tested for SA fires. A correlation analysis provided the basis for identifying the most significant controls on interannual variations in the number and average size of SA and non-SA fires.

We built empirical functions for the significant variables to diagnose the impact of fuel amount/continuity, flammability, and fire spread on both the number and size of fires at monthly intervals for SA fires (September–December) and non-SA fires (May–September) [*Pechony and Shindell*, 2009]. Preliminary analysis identified that regressions based on exponential relationships performed better than ones based on linear relationships. We built a total of four models (equations (1)–(4)) based on monthly records of climate and fire from 1959 to 2009. Variables were included sequentially based on the R square between inferred and observed monthly values adjusted by the degree of freedom.

The number of SA fires (NF_{sa}) for month m and year i was represented as

$$NF_{sa}(m,i) = C_1 \cdot e^{C_2 \cdot P_{cumu3}(m,i)} \cdot e^{-C_3 \cdot P(m,i)} \cdot e^{-C_4 \cdot RH_{sa}(m,i)} \cdot e^{C_5 \cdot E_{sa}(m,i)} \cdot \frac{1}{1 + e^{-(C_6 + C_7 \cdot S_{sa}(m,i))}} \quad (1)$$

where $C_{1,\ldots,7}$ are optimized coefficients, P_{cumu3} is the cumulative precipitation during the previous three winters, P is the monthly precipitation, RH_{sa} is the relative humidity during Santa Ana days, E_{sa} is the number of Santa Ana events, and S_{sa} is the fire spread in m s^{-1} calculated as a nonlinear function of wind speed on Santa Ana days [*Rothermel*, 1972; *Fosberg*, 1978]. The first term is related to previous herbaceous plant growth and thus fine fuel amount and continuity; the next two terms are related to fuel moisture; the final two terms are related to the occurrence and severity of Santa Ana events.

The mean size of SA fires (FS_{sa}), controlled by fuel drying and wind-driven spread, was represented as

$$FS_{sa}(m,i) = C_1 \cdot e^{-C_2 \cdot RH_{sa}(m,i)} \cdot e^{C_3 \cdot S_{sa}(m,i)} \quad (2)$$

We calculated the monthly burned area for the region as the product of fire number (equation (1)) and size (equation (2)).

The number of non-SA fires (NF_{nsa}) was represented as

$$NF_{nsa}(m,i) = C_1 \cdot e^{C_2 \cdot P_{cumu3}(m,i)} \cdot e^{-C_3 \cdot P(m-1,i)} \cdot e^{-C_4 \cdot RH(m,i)} \cdot \frac{1}{1 + e^{-(C_5 + C_6 \cdot T_{max}(m,i))}} \quad (3)$$

where $P(_{m-1})$ is the precipitation during the previous month and T_{max} is the average maximum temperature. The latter three terms in equation (3) are related to fuel flammability.

The average size of non-SA fires was represented as

$$FS_{nsa}(m,i) = C_1 \cdot e^{-C_2 \cdot P_{wet\&current}(m,i)} \cdot e^{-C_3 RH_{nsa}(m,i)} \cdot \frac{1}{1 + e^{-(C_4 + C_5 \cdot T_{max}(m,i))}} \cdot e^{C_6 \cdot S_{nsa}(m,i)} \quad (4)$$

where $P_{wet\&current}$ is the precipitation during the preceding wet season (winter and spring) and the current month precipitation; RH_{nsa} and S_{nsa} are the monthly relative humidity and fire spread [*Fosberg*, 1978] during days without Santa Ana winds. The first three terms in equation (4) are related to fuel drying.

We fit the models using the MatLab *fminsearch* function. We evaluated the performance of the optimized nonlinear models (equations (1) to (4)) using Pearson's correlation coefficients (r) and RMSE between inferred and observed fire at monthly, seasonal, and interannual intervals. We investigated the relative importance of each meteorological variable by normalizing the optimized model component containing each variable by its mean influence averaged over all months and years (hereafter each individual normalized model component is referred to as an influence function). We analyzed the correlation between the influence function for each weather variable and the number of fires and average fire size for each individual month. The magnitude and

©2014. American Geophysical Union. All Rights Reserved.

significance of correlation represents the strength of the relationship between an individual variable and fire, when all other controls were also considered in the optimized model.

3. Results

3.1. Spatial Distribution of Fires

An average of 41 fires greater than 40 ha occurred annually during 1959–2009, resulting in an average burned area of 53.3×10^3 ha per year. SA fires were usually larger than non-SA fires and occurred less frequently (Figure 2). The mean size of SA fires was 2691 ha, and the average number per year was 10. SA fires were clustered near high wind corridors that had severe fire weather indices during Santa Ana events (Figure 2a). This distribution is consistent with past work documenting that large fires during Santa Ana events occur most frequently in mountain passes and at locations with high offshore wind speeds [*Moritz et al.*, 2010].

Non-SA fires were widely distributed in foothill and mountain regions (Figure 2b). These fires were typically smaller, with a mean size of 882 ha, and more numerous than SA fires, accounting for 31 fires each year. The set of non-SA fires included a few large burns in remote mountain areas, including the Day (September 2006) and Zaca (July 2007) fires in Santa Barbara and northern Ventura counties, the Station fire (August 2009) in Los Angeles county, the Willow fire (August 1999) and the Sawtooth Complex fire (July 2006) in San Bernardino county, and the Pines fire (July 2002) in San Diego county.

The fire weather severity during the summer, as represented by the fire weather index, decreased markedly from the interior desert to the coast (Figure 2b). This gradient weakened during Santa Ana periods, with some coastal areas and mountain passes experiencing especially severe fire weather (Figure 2a). Similarly, the mean distance of fire perimeter centroids was closer to the coast for SA fires (41 ± 25 km from the coast) than non-SA fires (60 ± 29 km from the coast).

3.2. Seasonal Characteristics of Fires

Fires were most frequent in summer and fall (Figure 3). Spring and winter accounted for only 12% of the number of fires and 5% of annual burned area. About 24% of annual fires occurred during Santa Ana events (Figure 3a), accounting for nearly half of the annual burned area (49%; 25.9×10^3 ha per year) (Figure 3b). The majority of SA fires occurred in September through November; this period accounted for 72% of the total number of SA fires and 92% of the SA burned area. A key driver of this seasonality was the number of Santa Ana days, which increased from approximately 1 day per month in September to approximately 11 days per month in December (Figure 3f). Wind speed during Santa Ana events increased modestly from September to December (Figure 3h), but fuel flammability decreased with the onset of wet-season precipitation (Figure 3e) and decreasing relative humidity (Figure 3g). These offsetting effects caused SA fire number, size, and burned area to peak in October (Figures 3a–3c).

About 76% of fires were unrelated to Santa Ana events, accounting for half of the mean annual area burned (51%; 27.3×10^3 ha per year). Almost all of the fires from May to August, and half of the September burned area, were not associated with Santa Ana events. Non-SA fire activity peaked in July, coincident with especially low precipitation, low RH, and high air temperature, but also low wind speed (Figures 3d–3h).

Weather was typically drier (26% versus 45% RH) and windier (5 m s^{-1} versus 3 m s^{-1}) during Santa Ana periods compared with non-Santa Ana periods (Figures 3g and 3h). As a consequence, the Fosberg Fire Weather Index was more than twofold higher for SA fires (Figure 3i). This difference in fire weather was presumably the primary driver of the much larger fire sizes during Santa Ana events, especially in September and October. The mean fire size in October (approximately 4.6×10^3 ha per fire) was about fourfold larger than mean fire size in summer (Figure 3c).

3.3. Long-Term Trends and Interannual Variability

We did not find a significant multidecadal trend for the number, size, or burned area of SA fires (Figure 4). Firestorms in 1970, 2003, and 2007 led to larger fire sizes and greater burned areas in the 1970s and the 2000s (Figure 4b). In contrast, the average size of summer non-SA fires increased significantly each decade from approximately 1129 ha in the 1960s to 2121 ha in the 2000s (Figure 4b). This trend more than offset a concave downward decadal distribution of the number of non-SA fires (Figure 4a), resulting in a statistically significant increase in summer burned area (8299 ha $decade^{-1}$, 33% $decade^{-1}$, $p < 0.05$; Figure 4c). This trend was

©2014. American Geophysical Union. All Rights Reserved.

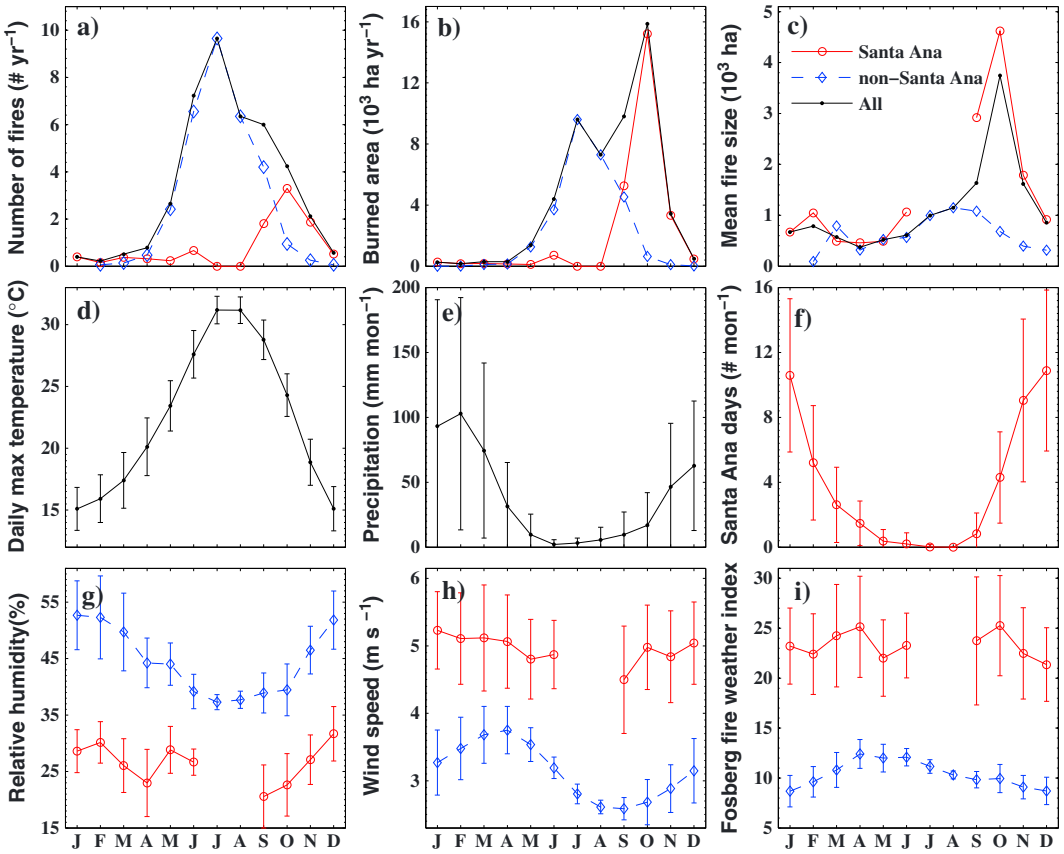

Figure 3. Seasonality of fire and weather averaged during 1959–2009 period. Temperature and precipitation were from PRISM, and other weather variables were from the extended MM5 climate model simulation forced with ERA-40 and North American Regional Reanalysis (NARR) boundary conditions. Monthly relative humidity, wind speed, and fire weather index were averaged during the identified Santa Ana and non-Santa Ana days separately.

mainly due to a significant increase in the number of fires greater than 2000 ha, from 18 in the 1960s and 13 in the 1970s to 28 in the 2000s.

Both fires and meteorological variables showed considerable year-to-year variability (Figures 5 and 6). The Mann-Kendall test [*Hirsch et al.*, 1982] confirmed that the number of annual summer non-SA fires (Sen's slope, 0.28 year^{-1}) and burned area (Sen's slope, 426 ha year^{-1}) increased significantly over the record ($p < 0.006$; Figure 5b). Summer T_{max} increased by approximately 1.0°C from 1959 to 2009 (Sen's slope, 0.02°C year^{-1}, $p < 0.01$) (Figure 6a). Other meteorological variables did not show significant long-term trends (Figures 6b–6e). No significant trend was found for the number and burned area of SA fires, though the average fire size increased marginally ($p = 0.07$) (Figure 5a). We did not find significant long-term trends for Santa Ana frequency or the RH or wind speed during Santa Ana events (Figures 6b, 6c, and 6e).

3.4. Controls on Santa Ana Fires

3.4.1. Number of SA Fires

The number of Santa Ana fires each year was negatively correlated with the average RH on Santa Ana days (Spearman correlation coefficient $r_s = -0.63$, $p < 0.001$) and positively correlated with the cumulative precipitation during the previous three winters ($r_s = 0.45$, $p < 0.001$) (Table 1). Other significant correlates included the number of Santa Ana events or Santa Ana days ($r_s = 0.38$), T_{max} ($r_s = 0.31$), precipitation during the current month ($r_s = -0.28$), and wind speed during Santa Ana days ($r_s = 0.28$). We used these five meteorological variables to construct an empirical model predicting the monthly number of SA fires (equation (1)). The influence functions for RH and current month precipitation were highly nonlinear (Figure S3).

©2014. American Geophysical Union. All Rights Reserved.

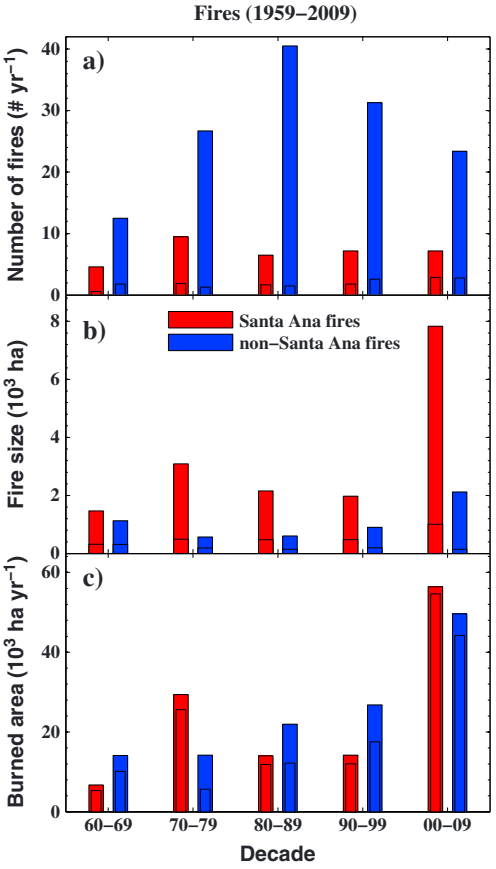

Figure 4. Decadal trends in (a) the number of fires, (b) mean fire size, and (c) burned area for Santa Ana fires (red) and non-Santa Ana fires (blue). Area burned increased steadily for summer non-SA fires, mostly contributed by fires greater than 2000 ha, as shown by the inside bars in Figures 4a and 4c. The medium fire size is shown as the horizontal line in Figure 4b.

The number of SA fires calculated with the model agreed reasonably well with the monthly observations on interannual (Figure 7a) and seasonal timescales (Figure 8), with a Pearson correlation coefficient (r) of 0.76 ($p < 0.001$) and RMSE of 2.3 for the 204 months from September to December over the 51 year period (Figure S4 and Table 2). The model diagnosed the large number of SA fires in 1970, 1985, 1993, 2003, and 2007, although the number of fires during some extreme years was underestimated. The optimized model explained much of the interannual variability for individual months (Figure S4). The performance varied among months, with the best agreement in September ($r = 0.85$), October ($r = 0.73$), and November ($r = 0.68$) at $p < 0.001$ (Table 2). The model correctly captured the October peak in SA fire number (Figure 8c). The decreasing fuel flammability from fall to winter with increasing RH and precipitation was counteracted most strongly by the increasing number of SA events and wind speed from September to December (Figure 8a).

The RH on Santa Ana days (from equation (1)) explained the largest amount of variability in the number of SA fires across all 204 months, as measured by the Pearson correlation ($r = 0.57$, $p < 0.001$) (Table 3). The other influence functions explained smaller amounts of the temporal variability but nonetheless improved the overall model fit. These functions included current precipitation ($r = 0.36$, $p < 0.001$), cumulative precipitation in the previous three winters ($r = 0.30$, $p < 0.001$), and fire spread rate ($r = 0.18$, $p < 0.05$) (Figure 7b and Table 3). The large number of SA

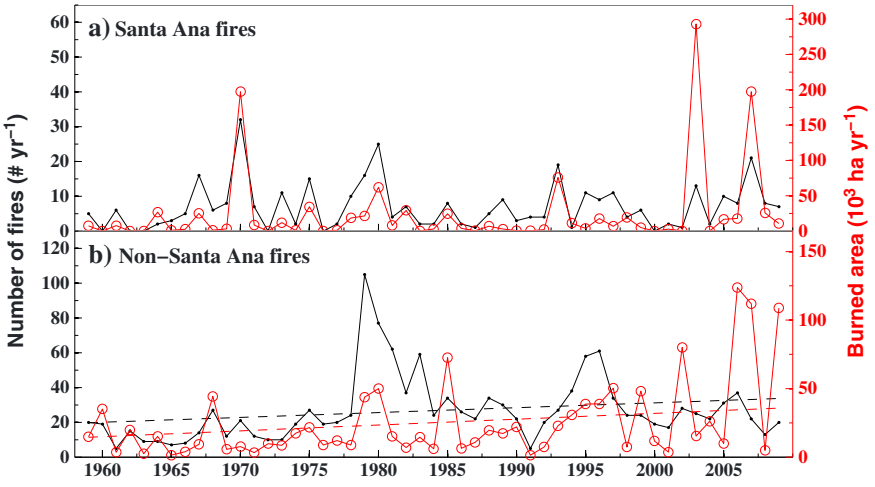

Figure 5. Time series of the number of fires and burned area for (a) Santa Ana fires during September–December and (b) non-Santa Ana fires during May–September. Significant linear trends are shown as dashed lines.

©2014. American Geophysical Union. All Rights Reserved.

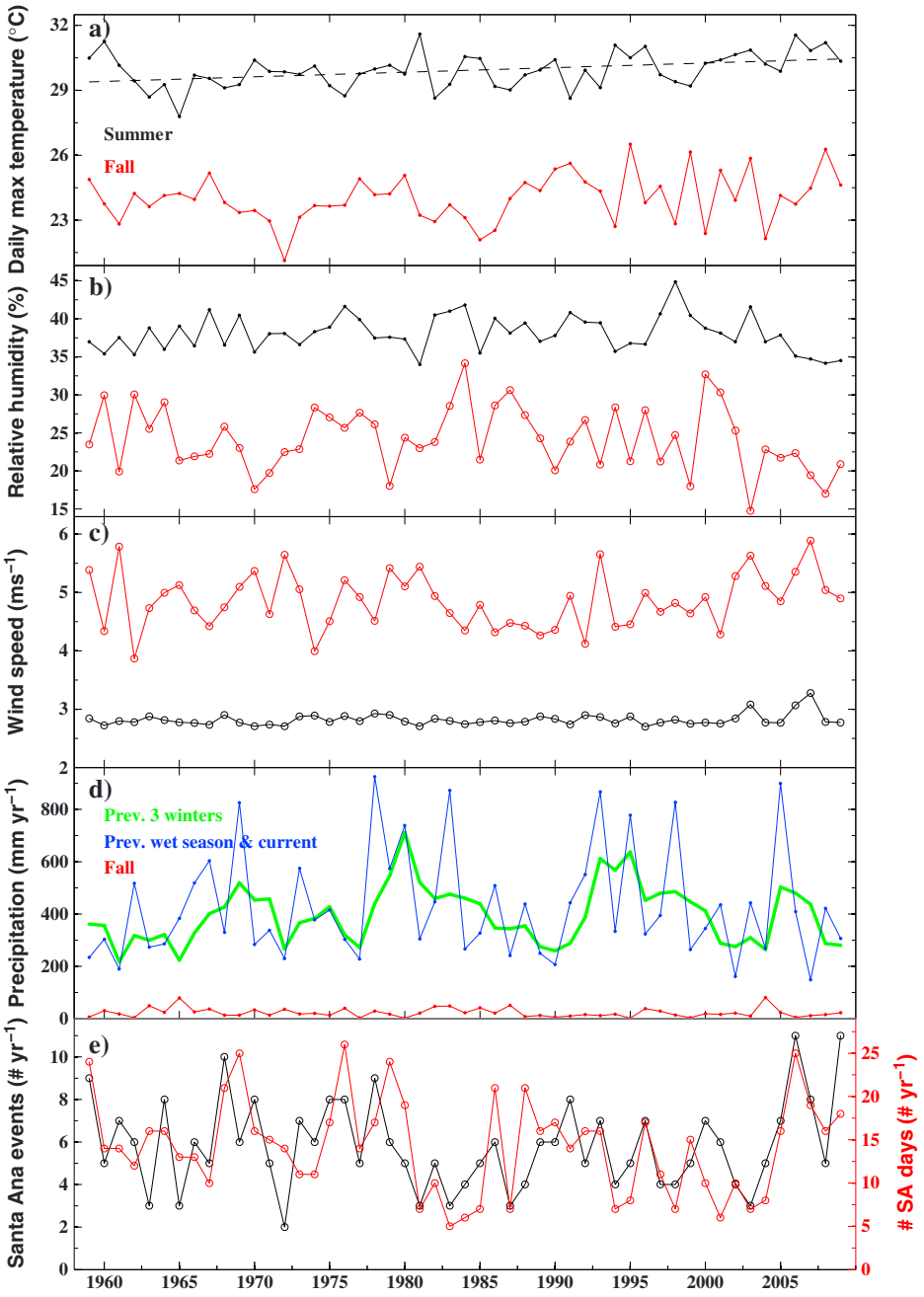

Figure 6. Time series of key meteorological drivers in summer (black) and fall (red). (a, b) Summer climate was the June–August average values weighted by the long term mean number of fires. (b) RH and (c) wind speed during the Santa Ana days from the extended MM5 data (open circle) were similarly averaged for fall September–November climate. (d) The cumulative precipitation from the previous three winters (October–March) is shown in green, and precipitation prior to summer fire season including precipitation from the previous wet season (winter and spring) and current month is shown in blue. (e) Annual number of Santa Ana events and days from September to November.

fires in 1970, 1979, 2003, and 2007 was mostly due to extremely low RHs in September and October (Figures 7b and S4). A combination of low RH and large antecedent precipitation contributed to large numbers of fires in November 1980 and October 1993 (Figure S4).

3.4.2. SA Fire Size

Wind speed and RH on Santa Ana days were significant predictors of seasonal and interannual variation of SA fire size (Tables 1 and 3 and Figure S5). The optimized model performed best for October fires ($r = 0.72$, $p < 0.0001$;

©2014. American Geophysical Union. All Rights Reserved.

Table 1. Spearman Correlation of Annual Santa Ana (SA) Fires (September–December) and Non-Santa Ana (Non-SA) Fires (May–September) With Meteorological Variables During 1959–2009

	Number of Fires				Burned Area				Average Fire Size			
	Non-SA Fires[a]		SA Fires[a]		Non-SA Fires[a]		SA Fires[a]		Non-SA Fires[a]		SA Fires[a]	
PRISM Meteorology[b]												
Mean temperature (T_{mean})	0.25	–[c]	0.18	–	0.33	**	0.03	–	0.25	–	−0.15	–
Maximum temperature (T_{max})	0.28	*	0.31	**	0.38	**	0.12	–	0.27	*	−0.22	–
Precipitation (PPT)	0.04	–	−0.28	*	−0.25	–	−0.19	–	−0.33	**	0.14	–
Winter precipitation (October–March)	0.19	–	0.35	**	−0.18	–	0.25	–	−0.36	**	0.06	–
Palmer Drought Severity Index	0.13	–	0.07	–	−0.28	*	−0.04	–	−0.47	***	0.04	–
Relative humidity (RH)	−0.06	–	−0.56	***	−0.40	***	−0.44	***	−0.44	***	0.13	–
Vapor pressure deficit	0.17	–	0.48	***	0.41	***	0.32	**	0.39	***	−0.17	–
Moisture damping factor[d]	0.05	–	0.55	***	0.40	***	0.41	***	0.45	***	−0.15	–
Previous three winter precipitation[e]	0.62	***	0.45	***	0.26	*	0.46	***	−0.11	–	0.31	–
Santa Ana Characteristics[b]												
# days			0.37	**			0.22	–			−0.08	–
# events			0.38	**			0.27	*			−0.04	–
Duration days			0.19	–			0.11	–			−0.07	–
Start day			−0.38	**			−0.29	*			0.15	–
Santa Ana Meteorology[b]												
Mean temperature (T_2)			0.26	–			0.23	–			−0.02	–
Relative humidity (RH)			−0.63	***			−0.46	***			−0.16	–
Fire spread[f]			0.28	*			0.32	**			0.41	**
Fosberg Fire Weather Index[g]			0.47	***			0.42	***			0.39	**
Non-Santa Ana Meteorology[b]												
Mean temperature (T_2)	0.04	–			0.20	–			0.20	–		
Relative humidity (RH)	−0.38	**			−0.46	***			−0.28	*		
Fire spread[f]	0.17	–			0.21	–			0.16	–		
Fosberg Fire Weather Index[g]	0.42	***			0.53	***			0.36	**		
Population[g]	0.43	***	0.18	–	0.36	**	0.19	–	0.12	–	0.31	–

[a]Two fire seasons were considered here: SA fires during September–December and non-SA fires during May–September.
[b]The monthly meteorological data during SA fire season was weighted by the long-term mean monthly number of SA fires to derive annual time series of seasonal meteorology (n = 51). Similar seasonal averaging was done for non-SA fire season. Santa Ana and non-Santa Ana meteorology was based on the monthly mean values of the merged MM5 and NARR data averaged over the Santa Ana days and non-Santa Ana days separately.
[c]Significance level: $p < 0.001$ (***), $p < 0.01$ (**), $p < 0.05$(*), and $p > 0.05$ (–, not significant).
[d]Moisture damping factor represents equilibrium moisture content as a function of relative humidity and temperature [*Fosberg*, 1978].
[e]Cumu3 PPT: cumulative precipitation from the previous three winters (October–March).
[f]Fire spread is a function of wind speed based on *Rothermel* [1972]. Fosberg Fire Weather Index (FFWI) is a product of moisture damping factor and fire spread [*Fosberg*, 1978].
[g]Population density was derived from RAND California population statistics, available at http://ca.rand.org/stats/popdemo/popdemo.html.

$n = 29$) (Figure S6) and agreed reasonably well with observations ($r = 0.56$, $p = 0.001$) for all 67 months when more than one SA fire was identified (Table 2 and Figure 7c). The RH influence function (from equation (2)) on Santa Ana days was the most important controller of the interannual variability in monthly SA fire size (Figures 7d and S6) and had a Pearson correlation of 0.46 ($p < 0.001$) with the time series of observed fire sizes (Table 3). The influence function for wind speed during Santa Ana days also was significant ($r = 0.30$, $p = 0.01$). The meteorological controls were the strongest for the interannual variation in October SA fire size, with correlation coefficients of 0.57 for RH and 0.54 for wind speed. The lowest RH (11.0%) during Santa Ana events occurred in October 2003; this coincided with a major firestorm and was significantly lower than the October Santa Ana mean (22.6 ± 5.5%) (Figure S6). Similarly, the RH on Santa Ana days in October 2007 was the third lowest observed during the entire record (14.5%). A large mean fire size observed in September 1970 coincided with RHs on Santa Ana days that were below average (13.5%) and wind speeds that were above average (5.9 m s^{-1}).

The optimized model partially captured the observed seasonal trends in fire size (Figure 8d). The simulated average SA fire size was greater than 2220 ha in September and October and decreased to 516 ha in December. The decreasing trend was caused by increasing RH from fall to winter. The result was a 77% decrease in the influence function of RH from September to December (Figure 8b), which was partly offset by 22% increase in the wind speed influence function.

©2014. American Geophysical Union. All Rights Reserved.

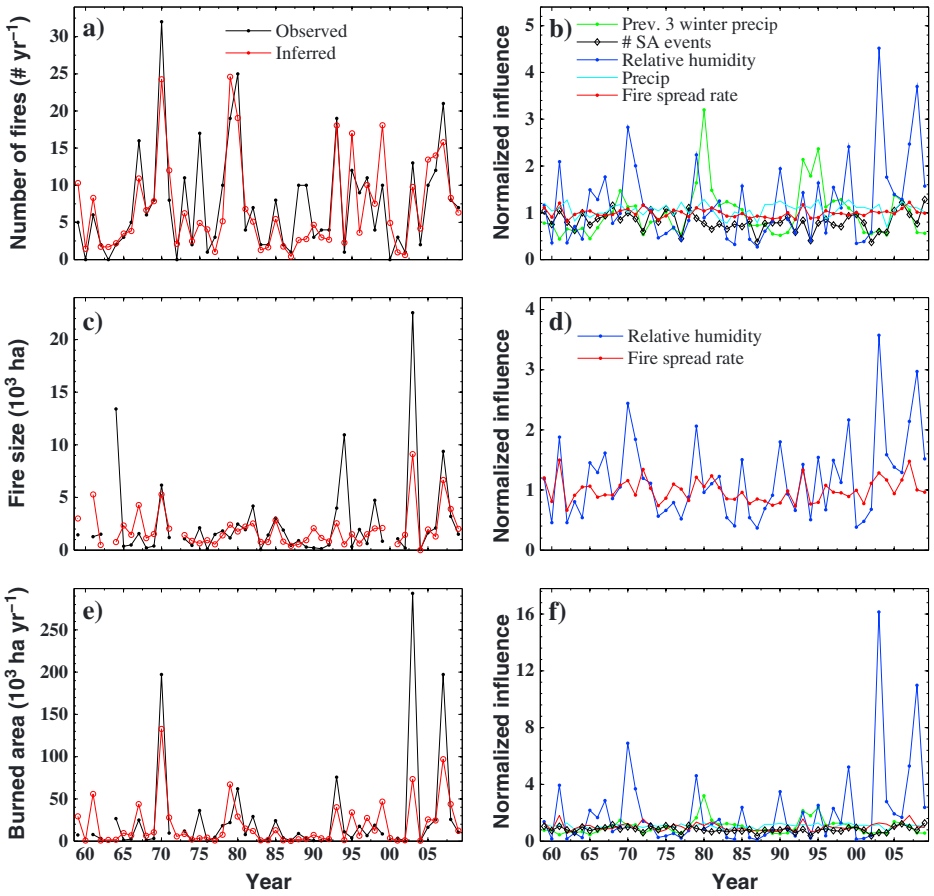

Figure 7. Time series of the observed and inferred (a) number of fires, (c) average fire size, and (e) burned area for Santa Ana fires during September–December. (b,d, and f) The influence functions for the meteorological driver variables are the monthly values (as shown in Figures S4 and S6) weighted by the long term mean number of Santa Ana fires.

3.4.3. SA Burned Area

The area burned during SA fires was significantly correlated with the RH on Santa Ana days ($r_s = -0.46$), the monthly mean RH ($r_s = -0.44$), the fire spread rate during SA events ($r_s = 0.32$), the number of SA events ($r_s = 0.27$), and the cumulative precipitation during the previous three winters ($r_s = 0.46$) (Table 1). The inferred total burned area, which was calculated as the product of the regression model estimates for the number of fires and the average fire size, captured the peaks in burned area during the 1970, 2003, and 2007 firestorms and agreed well with the observed burned area ($r = 0.76$, $p < 0.001$) (Figures 7e and S7 and Table 2). The RH on Santa Ana days was the dominant control of burned area (Figure 7f).

3.5. Controls on Non-Santa Ana Fires

3.5.1. Number of Non-SA Fires

The cumulative precipitation during the previous three winters was highly correlated with the number of May–September non-SA fires ($r_s = 0.62$, $p < 0.01$; $n = 51$). RH on non-Santa Ana days ($r_s = -0.38$, $p = 0.01$) and T_{max} ($r_s = 0.28$, $p = 0.05$) also were important correlates (Table 1). Precipitation during the previous month significantly improved the estimate of the number of non-SA fires at monthly time scales (equation (3)). The optimization (Figure S3) showed that cumulative precipitation from the previous three winters and T_{max} had similar levels of influence within the model (Table 3). The influence functions for RH and previous month precipitation were approximately linear and much weaker than those for SA fires (Figure S3 and Tables 1 and 3).

The inferred number of non-SA fires from the regression model (equation (3)) was in good agreement with the monthly observations from May to September over 51 years ($r = 0.60$, $p < 0.001$; RMSE = 5.4; $n = 255$) (Figure S8 and Table 2). The model captured much of the interannual variability for individual months (Figure S8) and

©2014. American Geophysical Union. All Rights Reserved.

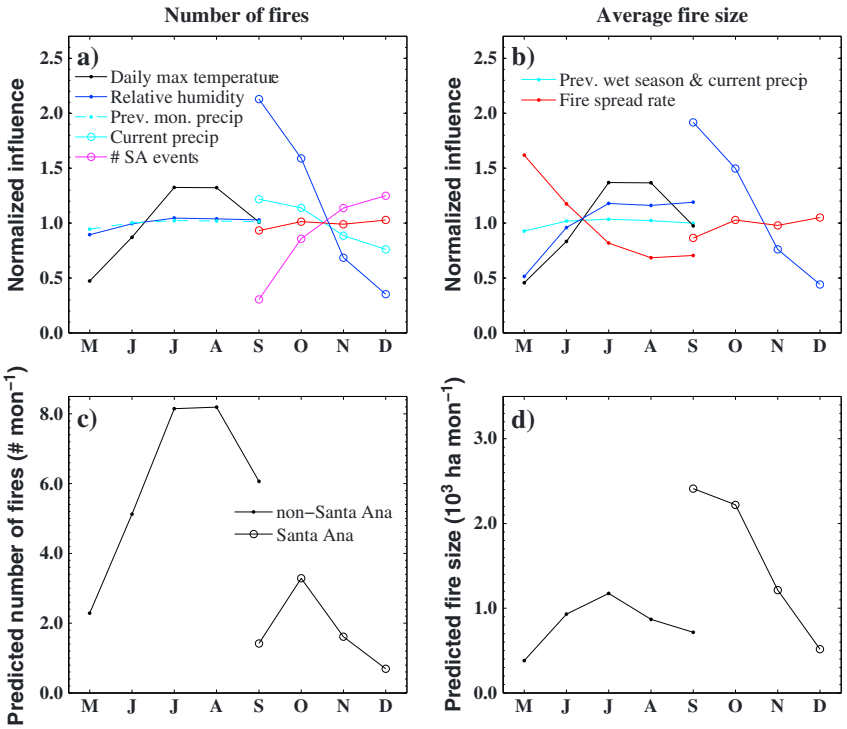

Figure 8. Seasonality of the influence functions for the primary climate variables for (a) the number of fires and (b) mean fire size for September–December Santa Ana fires (open circle) and May–September non-Santa Ana fires (solid circle). (c and d) The inferred seasonal cycles.

for the summer fire season (Figure 9a). The best performance was found for July ($r = 0.74$) (Figure S8 and Table 2). The model also captured the seasonal patterns of non-Santa Ana fires (Figure S8 and Figure 8c). T_{max} was the primary variable driving the seasonal variation in the number of fires (Figure 8a).

All four variables in the model (equation (3)) were significant in controlling the month-to-month and interannual variability ($p < 0.001$) (Table 3). The influence function for cumulative precipitation during the previous three winters dominated the overall interannual variability ($r = 0.40$) (Figures 9b and S8 and Table 3). Summers with particularly large numbers of non-SA fires, especially in June and July, followed unusually wet winters (e.g., in 1980 and 1995; Figure S8 and 9a). The T_{max} influence function also contributed significantly to the model's ability to capture temporal variability in the number of fires ($r = 0.39$); RH ($r = 0.31$) and previous month precipitation ($r = 0.21$) were less important. On interannual time scales, the influence from cumulative precipitation during the three previous winters was highest in July ($r = 0.67$) and considerably weaker in the earlier months (Table 3). Controls by T_{max} were dominant in May ($r = 0.54$) and June ($r = 0.45$) and less important in July and August.

3.5.2. Average Non-SA Fire Size

Interannual variability in non-SA fire size during May–September correlated significantly with PDSI ($r_s = -0.47$, $p < 0.001$), seasonal PRISM RH ($r_s = -0.44$, $p < 0.001$), previous winter precipitation ($r_s = -0.36$, $p < 0.01$), and current precipitation ($r_s = -0.33$, $p = 0.02$) (Table 1). T_{max} was moderately correlated with non-SA fire size ($r_s = 0.27$, $p = 0.05$). Wind speed affected fire size in some months (especially July; data not shown).

We used RH, T_{max}, wind speed, and recent precipitation ($P_{wet\&current}$) as predictors in our fire size model (equation (4) and Figure S5). A total of 189 months when more than one fire was identified were used for optimization (Figure S9). The optimized model captured both seasonal (Figure 8d) and interannual (Figure 9c) variability in observed fire size, as shown by an overall Pearson's correlation of 0.36 ($p < 0.001$) (Table 2). Model performance was highest in July ($r = 0.64$, $p < 0.001$; $n = 48$) (Figure S9). The inferred fire size increased from 381 ha in May to 1175 ha in July (Figure 8d) and was consistent with the observed seasonality (Figure 3c). Increasing T_{max} and decreasing RH from late spring to late summer were counterbalanced by decreasing wind speed (Figure 8b); the result was a maximum fire size in July (Figure 8d).

©2014. American Geophysical Union. All Rights Reserved.

Table 2. Performance of Optimized Models for Predicting the Number of Fires, Fire Size, and Total Burned Area for Santa Ana Fires and Non-Santa Ana Fires

	Number of Fires				Fire Size[a] (10^3 ha)				Burned Area (10^3 ha)			
	# Observation	Pearson Correlation[b]		RMSE	# Observation	Pearson Correlation[b]		RMSE	# Observation	Pearson Correlation[b]		RMSE
Non-Santa Ana Fires												
May	51	0.64	***	2.9	22	0.18	–	1.1	51	0.56	***	2.6
Jun	51	0.60	***	7.3	38	0.31	*	1.5	51	0.48	***	11.2
Jul	51	0.74	***	7.1	48	0.64	***	2.0	51	0.79	***	10.5
Aug	51	0.55	***	4.3	46	0.31	*	1.3	51	0.13	–	17.5
Sep	51	0.60	***	3.6	35	0.32	*	2.3	51	0.37	**	9.6
All	255	0.60	***	5.4	189	0.36	***	1.7	255	0.47	***	11.3
Santa Ana Fires												
Sep	51	0.85	***	2.2	14	0.36	–	2.6	51	0.82	***	25.3
Oct	51	0.73	***	2.9	29	0.72	***	3.3	51	0.77	***	43.2
Nov	51	0.68	***	2.4	18	0.02	–	1.9	51	0.39	*	10.9
Dec	51	0.16	–	1.2	6	0.01	–	0.7	51	0.20	–	2.5
All	204	0.76	***	2.3	67	0.56	***	2.7	204	0.76	***	29.4

[a]Months when less than two fires were identified were not included for fire size regression model.
[b]Significance level: $p < 0.001$ (***), $p < 0.01$ (**), $p < 0.05$(*), and $p > 0.05$ (–, not significant).

Table 3. Relative Importance of the Primary Meteorological Drivers in Controlling the Interannual Variability in Fire Number and Size, as Measured Using Pearson Correlation Coefficients With the Optimized Meteorological Influence Functions

Number of Fires (Pearson Correlation and Significance)															
Non-Santa Ana Fires	# observation	$f(PPT_{cumu3})$[a]		$f(T_{max})$		f(RH)		f(PPT)						$f(PPT_{cumu3})\cdot f$(RH)	
May	51	0.15	–[b]	0.54	***	0.44	***	0.27	*					0.31	*
Jun	51	0.35	**	0.45	***	0.42	***	0.08	–					0.45	***
Jul	51	0.67	***	0.24	–	0.06	–	0.03	–					0.70	***
Aug	51	0.52	***	0.24	–	0.09	–	0.03	–					0.52	***
Sep	51	0.54	***	0.35	**	0.18	–	0.07	–					0.55	***
All month years	255	0.40	***	0.39	***	0.31	***	0.21	***					0.49	***
Santa Ana Fires	# observation	$f(PPT_{cumu3})$[a]				f(RH)		f(PPT)		f(# SA events)		f(Wind)		f(RH)·f(Wind)	
Sep	51	0.11	–			0.39	–	0.12	–	0.58	***	0.29	–	0.39	–
Oct	51	0.29	*			0.58	***	0.29	*	0.27	*	0.38	**	0.64	***
Nov	51	0.57	***			0.43	***	0.30	*	0.07	–	0.24	–	0.40	***
Dec	51	0.04	–			−0.02	–	0.19	–	−0.01	–	0.01	–	−0.03	–
All month years	204	0.30	***			0.57	***	0.36	***	−0.16	*	0.18	**	0.58	***

Fire Size[c] (Pearson Correlation and Significance)											
Non-Santa Ana Fires	# observation	$f(T_{max})$		f(RH)		$f(P_{wet\&current})$[d]		f(Wind)		f(RH)·f(Wind)	
May	22	0.05	–	0.10	–	0.32	–	0.21	–	0.22	–
Jun	38	0.25	–	0.21	–	0.35	*	0.14	–	0.20	–
Jul	48	0.25	–	0.17	–	0.42	***	0.59	***	0.52	***
Aug	46	0.06	–	0.48	***	0.05	–	0.02	–	0.46	***
Sep	35	0.02	–	0.36	*	0.19	–	0.26	–	0.33	*
All month years	189	0.15	*	0.28	***	0.24	***	0.02	–	0.21	***
Santa Ana Fires	# observation			f(RH)				f(Wind)		f(RH)·f(Wind)	
Sep	14			0.26	–			0.31	–	0.36	–
Oct	29			0.57	***			0.54	**	0.72	***
Nov	18			0.00	–			0.04	–	0.02	–
Dec	6			−0.34	–			0.51	–	0.01	–
All month years	67			0.46	***			0.30	**	0.56	***

[a]PPT_{cumu3} represents the cumulative precipitation from the previous three winters.
[b]Significance level: $p < 0.001$ (***), $p < 0.01$ (**), $p < 0.05$(*), and $p > 0.05$ (–, not significant).
[c]An individual month year was included when more than one fire was identified.
[d]$P_{wet\&current}$ represents the cumulative precipitation from the preceding winter and spring (October–April) and precipitation during the current month. For summer season, it mainly captures the precipitation from the preceding wet season, since precipitation probability is very low from June to September.

©2014. American Geophysical Union. All Rights Reserved.

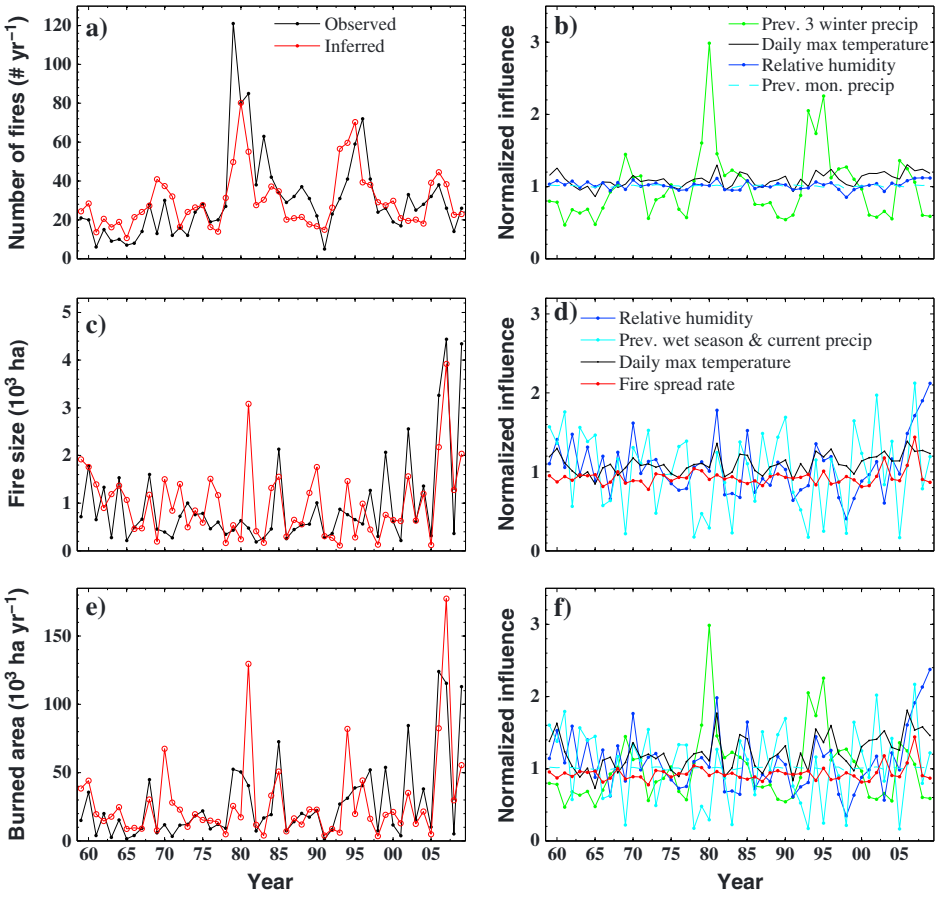

Figure 9. Similar as Figure 7, but for non-Santa Ana fires during May–September. Monthly values are shown in Figures S8 and S9.

RH was the most significant variable in explaining interannual non-SA fire size variability, with an overall Pearson's correlation coefficient of 0.28 ($p < 0.001$, $n = 189$). $P_{wet\&current}$ ($r = 0.24$, $p < 0.001$) and T_{max} ($r = 0.15$, $p < 0.05$) were also important (Table 3 and Figure S9). The relative importance of the climate variable influence functions varied between months (Table 3 and Figure S9). The RH influence function affected the interannual variability in August and September non-SA fire sizes significantly. The influence function for precipitation during the previous wet season and current month was significant in May–July, and the T_{max} influence was only significant in June. Both precipitation and temperature influence functions became less important in August and September, when soil was typically dry and the weather was hot. The influence of wind speed on fire size was only significant in July ($r = 0.59$, $p < 0.0001$).

3.5.3. Non-SA Burned Area

The inferred total burned area for non-SA summer fires agreed well with the observed time series (Figure 9e), with a $r = 0.47$ for all 255 May–September months. The best prediction of burned area was found for July ($r = 0.79$, $p < 0.001$) (Table 2 and Figure S10). The average T_{max}, mean RH, and cumulative precipitation from the previous three winters each contributed to the interannual variation of summer burned area (Figure 9f and Table 1).

4. Discussion

Wildland fires are common in Southern California, and most of the natural vegetation is well adapted to periodic crown fire [*Barbour et al.*, 2007]. We partitioned historical burn perimeters into Santa Ana and non-Santa Ana fires and quantified the impacts of meteorological conditions on the two types of fire. We found that meteorological variables explained 57% of the temporal variability in burned area for SA fires and 22% for non-SA fires.

©2014. American Geophysical Union. All Rights Reserved.

4.1. Contrasting Controls on SA and Non-SA Fires

Separate analysis indicated that both fire weather and fuel continuity exert important controls on the seasonal and interannual patterns of SA and non-SA fire number, though the relative importance of these controls varied with fire type. Above average precipitation during the previous three winters enhanced the number of fires, and this effect was most pronounced for non-SA fires during June to September (Tables 1 and 3). We hypothesize that higher precipitation over several years promotes the growth of grass and other herbaceous vegetation, which leads to an accumulation of fine fuel [*Swetnam and Betancourt*, 1998; *Westerling et al.*, 2011]. An increase in fine fuel density also increases the continuity between adjacent wildlands and areas with frequent human activity, including roads and houses. A buildup of fine litter following one or more wet growing season likely increases the probability that fires will escape from settlement areas into more interior shrublands. The continuity of fine fuel is particularly important in Southern California, where many fires originate along traffic corridors and in areas with immediate road access [*Faivre et al.*, 2014]. Grass production is very sensitive to precipitation in California [*Jin and Goulden*, 2013], and wet years should lead to increased fine fuel loads. Aboveground dead grass typically takes a couple of years to decompose completely [*Parton et al.*, 2007]. The large number of summer fires in 1980 followed several wet winters associated with the 1977–1978 ENSO; the large number of fires in 1995 followed the 1991–1995 ENSO [e.g., *Castello and Shelton*, 2004].

Immediate fire weather was more important than the amount and continuity fine fuel in determining the number of SA fires (Table 3). The weather during fall and winter Santa Ana events was extreme; RH was at least 10% lower, and wind speed at least 1.5 m s^{-1} higher, during SA events compared to summer conditions (Figure 3). Extremely low RH and strong winds dry fuel [*Viney*, 1991] enhance fire spread and increase ignition risk (e.g., by blowing down trees into power lines). RH was an especially important predictor of year-to-year SA fire variation. It was only weakly correlated with the wind speed during Santa Ana days ($r = -0.27$) and had more significant temporal variability (coefficient of variance: 25%) than that of wind speed (coefficient of variance: 14%). RH during Santa Ana days explained 32% of the temporal variability in the number of SA fires, 21% of the variability in fire size, and 36% of the temporal variability in burned area (Table 3).

Precipitation during the current month had a significant negative effect on SA fire number by affecting fuel flammability, and recent precipitation during the preceding wet season and current month had a significant negative effect on summer fire size. Dry winters and springs reduce live fuel moisture early in the early fire season [*Dennison et al*., 2008]. Drought, especially over several years, also reduces leaf area [*Kimball et al.*, 2013] and causes shrub and tree mortality [*Kelly and Goulden*, 2008]. The maximum flame height for dead shrub fuel is usually increased relative to that for live shrubs [*Sun et al*., 2006]. The ratio of live to dead fuel and the moisture content of live fuel may be more important for fire spread under moderate weather conditions in summer than during fall Santa Ana events.

4.2. Implications for Fire Management and Planning

Santa Ana and non-Santa Ana fires exhibit distinct spatial patterns and behavior, opening the possibility of further targeting management strategy based on local fire regime [*Reinhardt et al.*, 2008]. Meteorological conditions explained 57% of the interannual variation in SA burned area and 22% of the interannual variation in non-SA burned area (Table 2); the remaining variability is presumably controlled in part by other factors, such as ignition, suppression, management, topography, and burn history. The greater importance of meteorology in explaining SA fires relative to non-SA fires implies that nonmeteorological factors are comparatively more important for non-SA fires (Tables 1 and 3). The effectiveness of fire suppression depends on weather, access, and terrain; effective and safe suppression is often impossible during Santa Ana conditions. Similarly, the dominant effect of meteorology on Santa Ana fires calls into question efforts to reduce autumn fires by fuel management [*Keeley et al*., 1999]. In contrast, the immediate meteorology is less important (and fuels are relatively more important) for non-Santa Ana fires, suggesting that fuel management targeted at reducing summer, non-SA fires may prove comparatively useful [*Minnich*, 1983; *Reinhardt et al.*, 2008; *Schoennagel et al.*, 2009].

Similarly, it may also be possible to tailor fire weather forecasts based on the two types of fire. The US National Weather Service issues fire weather alerts to warn agencies and residents of conditions conductive to increased wildfire activity; the associated criteria include the duration of low RH, wind strength, and fuel moisture (http://www.fire.ca.gov/communications). Our analysis indicates different criteria may be appropriate for SA

©2014. American Geophysical Union. All Rights Reserved.

and non-SA fires. Information on fuel amount and condition (fuel connectivity, dead-to-live ratio, fuel moisture, and green-up) is more likely to be useful for anticipating summer fires. Increased fine fuel amount and continuity, based on cumulative precipitation during the previous 2 to 3 years, may indicate an increased probability of a larger number of summer fires, whereas a dry preceding winter may provide early signs for larger average fire size.

4.3. Implications for Predicting Future Fires

Most climate models project a warmer and drier climate in California by year 2100 [*Cayan et al.*, 2008; *Cayan et al.*, 2010]. Recent assessments of the impact of climate change on Southern California Santa Ana events indicate reduced SA frequency [*Miller and Schlegel*, 2006; *Hughes et al.*, 2011] and increased intensity (e.g., lower RH and higher temperature) [*Hughes et al.*, 2011]. A decrease in the frequency of Santa Ana events should reduce SA fire frequency, especially at the beginning of the Santa Ana season in September. However, reduced RH during Santa Ana periods or a later start to the fall and winter precipitation season will likely increase the probability of ignition success and the rate of fire spread. Moreover, our study implies that non-Santa Ana fires are likely to increase during summer with future warming and possible RH decrease [*Cayan et al.*, 2008; *Franco et al.*, 2011; *Pierce et al.*, 2013]. In fact, the increasing trend in summer fires we observed (Figure 5) may be linked to increasing summer temperatures in the region (Figure 6).

The majority of fires in Southern California are started by humans [*Syphard et al.*, 2007], and a critical question is whether increasing population density and proximity to wild areas will increase ignition probability [*Faivre et al.*, 2014]. Future studies are needed to examine how ignition will evolve spatially and temporally with population growth and development, and how fire fighting strategies and fuel management affect fire size for the two contrasting types of fires.

Acknowledgments
This research was supported by NASA grant NNX10AL14G. We thank the NARR project for making the NARR reanalysis publicly available, and the MM5 model community. We are also grateful for the valuable comments from Baldocchi and two anonymous reviewers.

References

Abatzoglou, J. T., R. Barbero, and N. J. Nauslar (2013), Diagnosing Santa Ana winds in Southern California with synoptic-scale analysis, *Wea. Forecast.*, *28*(3), 704–710, doi:10.1175/WAF-D-13-00002.1.

Balch, J. K., B. A. Bradley, C. M. D'Antonio, and J. Gomez-Dans (2013), Introduced annual grass increases regional fire activity across the arid western USA (1980–2009), *Glob. Change Biol.*, *19*(1), 173–183, doi:10.1111/gcb.12046.

Barbour, M., T. Keeler-Wolf, and A. A. Schonenderr (Eds) (2007), *Terrestrial Vegetation of California*, 3rd ed., Univ. of California Press, California.

Bartlein, P. J., S. W. Hostetler, S. L. Shafer, J. O. Holman, and A. M. Solomon (2008), Temporal and spatial structure in a daily wildfire-start data set from the western United States (1986–96), *Int. J. Wildland Fire*, *17*(1), 8–17, doi:10.1071/WF07022.

Brown, T. J., B. L. Hall, and A. L. Westerling (2004), The impact of twenty-first century climate change on wildland fire danger in the western United States: An applications perspective, *Clim. Change*, *62*(1–3), 365–388.

California Department of Forestry and Fire Protection—The Fire and Resource Assessment Program (CDF-FRAP) (2012), Statewide geodatabase with wildfire history current as of 2012. [Available at http://frap.cdf.ca.gov/projects/fire_data/fire_perimeters/.]

Castello, A. F., and M. L. Shelton (2004), Winter precipitation on the US Pacific coast and El Nino–southern oscillation events, *Int. J. Climatol.*, *24*(4), 481–497, doi:10.1002/joc.1011.

Cayan, D. R., E. P. Maurer, M. D. Dettinger, M. Tyree, and K. Hayhoe (2008), Climate change scenarios for the California region, *Clim. Change*, *87*, S21–S42, doi:10.1007/s10584-007-9377-6.

Cayan, D. R., T. Das, D. W. Pierce, T. P. Barnett, M. Tyree, and A. Gershunov (2010), Future dryness in the southwest US and the hydrology of the early 21st century drought, *Proc. Natl. Acad. Sci. U.S.A.*, *107*(50), 21,271–21,276, doi:10.1073/pnas.0912391107.

Conil, S., and A. Hall (2006), Local regimes of atmospheric variability: A case study of Southern California, *J. Clim.*, *19*(17), 4308–4325, doi:10.1175/JCLI3837.1.

Daly, C., M. Halbleib, J. I. Smith, W. P. Gibson, M. K. Doggett, G. H. Taylor, J. Curtis, and P. P. Pasteris (2008), Physiographically sensitive mapping of climatological temperature and precipitation across the conterminous United States, *Int. J. Climatol.*, *28*(15), 2031–2064, doi:10.1002/joc.1688.

Davis, F. W., and J. C. Michaelson (1995), Sensitivity of fire regime in chaparral ecosystems to global climate change, in *Global Change and Mediterranean-type Ecosystems*, edited by J. M. Moreno and W. C. Oechel, pp. 203–224, Springer, New York.

Delfino, R. J., et al. (2009), The relationship of respiratory and cardiovascular hospital admissions to the southern California wildfires of 2003, *Occup. Environ. Med.*, *66*(3), 189–197, doi:10.1136/oem.2008.041376.

Dennison, P. E., M. A. Moritz, and R. S. Taylor (2008), Evaluating predictive models of critical live fuel moisture in the Santa Monica Mountains, California, *Int. J. Wildland Fire*, *17*(1), 18–27, doi:10.1071/Wf07017.

Faivre, N., Y. Jin, M. L. Goulden, and J. T. Randerson (2014), Controls on the spatial pattern of wildfire ignitions in Southern California, *Int. J. Wildland Fire*, under review.

Fosberg, M. A. (1978), Weather in wildland fire management: The fire weather index, paper presented at *Conference on Sierra Nevada Meteorology*, *American Meteorological Society*, Lake Tahoe, California.

Franco, G., D. R. Cayan, S. Moser, M. Hanemann, and M. A. Jones (2011), Second California Assessment: Integrated climate change impacts assessment of natural and managed systems, *Clim. Change*, *109*, 1–19, doi:10.1007/S10584-011-0318-Z.

Gershunov, A., T. P. Barnett, D. R. Cayan, T. Tubbs, and L. Goddard (2000), Predicting and downscaling ENSO impacts on intraseasonal precipitation statistics in California: The 1997/98 event, *J. Hydrometeorol.*, *1*(3), 201–210, doi:10.1175/1525-7541.

Grell, G. A., J. Dudhia, and D. R. Stauffer (1995), *A Description of the Fifth-Generation Penn State/NCAR Mesoscale Model (MM5), NCAR/TN-398*, Boulder, CO., NCAR.

Halsey, R. W. (Ed) (2005), *Fire, Chaparral, and Survival in Southern California*, Sunbelt Publications, San Diego, Calif.

©2014. American Geophysical Union. All Rights Reserved.

Hirsch, R. M., J. R. Slack, and R. A. Smith (1982), Techniques of trend analysis for monthly water quality data, *Water Resour. Res.*, *18*(1), 107–121, doi:10.1029/WR018i001p00107.
Hughes, M., and A. Hall (2010), Local and synoptic mechanisms causing Southern California's Santa Ana winds, *Clim. Dynam.*, *34*(6), 847–857, doi:10.1007/S00382-009-0650-4.
Hughes, M., A. Hall, and J. Kim (2011), Human-induced changes in wind, temperature and relative humidity during Santa Ana events, *Clim. Change*, *109*, 119–132, doi:10.1007/S10584-011-0300-9.
Jin, Y., and M. L. Goulden (2013), Ecological consequences of variation in precipitation: Separating short- vs. long-term effects using satellite data, *Global Ecol. Biogeogr.*, *23*(3), doi:10.1111/geb.12135.
Keeley, J. E., C. J. Fotheringham, and M. Morais (1999), Reexamining fire suppression impacts on brushland fire regimes, *Science*, *284*(5421), 1829–1832, doi:10.1126/science.284.5421.1829.
Keeley, J. E., and P. H. Zedler (2009), Large, high-intensity fire events in southern California shrublands: Debunking the fine-grain age patch model, *Ecol. Appl.*, *19*(1), 69–94, doi:10.1890/08-0281.1.
Keeley, J. E. (2004), Impact of antecedent climate on fire regimes in coastal California, *Int. J. Wildland Fire*, *13*(2), 173–182, doi:10.1071/WF03037.
Keeley, J. E., C. J. Fotheringham, and M. A. Moritz (2004), Lessons from the October 2003 wildfires in Southern California, *J. Forest.*, *102*(7), 26–31.
Keeley, J. E., H. Safford, C. J. Fotheringham, J. Franklin, and M. Moritz (2009), The 2007 Southern California wildfires: Lessons in complexity, *J. Forest.*, *107*(6), 287–296.
Kelly, A. E., and M. L. Goulden (2008), Rapid shifts in plant distribution with recent climate change, *Proc. Natl. Acad. Sci. U.S.A.*, *105*(33), 11,823–11,826, doi:10.1073/pnas.0802891105.
Kimball, J. S., S. W. Running, and R. Nemani (1997), An improved method for estimating surface humidity from daily minimum temperature, *Agric. Forest Meteorol.*, *85*, 87–98.
Kimball, S., M. Goulden, K. N. Suding, and S. Parker (2013), Altered water and nitrogen input shifts succession in a Southern California coastal sage community, *Eco. Appl.*, doi:10.1890/13-1213.1.
Krawchuk, M. A., and M. A. Moritz (2011), Constraints on global fire activity vary across a resource gradient, *Ecology*, *92*(1), 121–132, doi:10.1890/09-1843.1.
Littell, J. S., D. McKenzie, D. L. Peterson, and A. L. Westerling (2009), Climate and wildfire area burned in western U. S. ecoprovinces, 1916–2003, *Ecol. Appl.*, *19*(4), 1003–1021, doi:10.1890/07-1183.1.
Mesinger, F., et al. (2006), North American regional reanalysis, *Bull. Am. Meteorol. Soc.*, *87*(3), 343–360, doi:10.1175/BAMS-87-3-343.
Miller, N. L., and N. J. Schlegel (2006), Climate change projected fire weather sensitivity: California Santa Ana wind occurrence, *Geophys. Res. Lett.*, *33*, L15711, doi:10.1029/2006gl025808.
Minnich, R. A. (1983), Fire mosaics in Southern California and Northern Baja California, *Science*, *219*(4590), 1287–1294, doi:10.1126/science.219.4590.1287.
Minnich, R. A. (2001), An integrated model of two fire regimes, *Conserv. Biol.*, *15*(6), 1549–1553, doi:10.1046/J.1523-1739.2001.01067.X.
Mo, K. C., and R. W. Higgins (1998), Tropical influences on California precipitation, *J. Clim.*, *11*(3), 412–430, doi:10.1175/1520-0442.
Moritz, M. A., T. J. Moody, M. A. Krawchuk, M. Hughes, and A. Hall (2010), Spatial variation in extreme winds predicts large wildfire locations in chaparral ecosystems, *Geophys. Res. Lett.*, *37*, L04801, doi:10.1029/2009gl041735.
Morton, D. C., G. J. Collatz, D. Wang, J. T. Randerson, L. Giglio, and Y. Chen (2013), Satellite-based assessment of climate controls on US burned area, *Biogeosciences*, *10*(1), 247–260, doi:10.5194/bg-10-247-2013.
Parton, W., et al. (2007), Global-scale similarities in nitrogen release patterns during long-term decomposition, *Science*, *315*(5810), 361–364, doi:10.1126/science.1134853.
Pausas, J. G. (2004), Changes in fire and climate in the eastern Iberian Peninsula (Mediterranean basin), *Clim. Change*, *63*(3), 337–350, doi:10.1023/B:CLIM.0000018508.94901.9c.
Pausas, J. G., and S. Paula (2012), Fuel shapes the fire-climate relationship: Evidence from Mediterranean ecosystems, *Global Ecol. Biogeogr.*, *21*(11), 1074–1082, doi:10.1111/j.1466-8238.2012.00769.x.
Pausas, J. G., and E. Ribeiro (2013), The global fire-productivity relationship, *Global Ecol. Biogeogr.*, *22*(6), 728–736, doi:10.1111/geb.12043.
Pechony, O., and D. T. Shindell (2009), Fire parameterization on a global scale, *J. Geophys. Res.*, *114*, D16115, doi:10.1029/2009jd011927.
Pierce, D. W., A. L. Westerling, and J. Oyler (2013), Future humidity trends over the western United States in the CMIP5 global climate models and variable infiltration capacity hydrological modeling system, *Hydrol. Earth Syst. Sci.*, *17*, 1833–1850, doi:10.5194/hess-17-1833-2013.
Reinhardt, E. D., R. E. Keane, D. E. Calkin, and J. D. Cohen (2008), Objectives and considerations for wildland fuel treatment in forested ecosystems of the interior western United States, *Forest Ecol. Manag.*, *256*(12), 1997–2006, doi:10.1016/j.foreco.2008.09.016.
Rothermel, R. C. (1972), A mathematical model for predicting fire spread in wildland fuels, in *Intermountain Forest and Range Experiment Station Research Paper*, INT-115, pp. 40, USDA Forest Service, Ogden, UT.
Schoennagel, T., C. R. Nelson, D. M. Theobald, G. C. Carnwath, and T. B. Chapman (2009), Implementation of National Fire Plan treatments near the wildland-urban interface in the western United States, *Proc. Natl. Acad. Sci. U.S.A.*, *106*(26), 10,706–10,711, doi:10.1073/pnas.0900991106.
Schonher, T., and S. E. Nicholson (1989), The relationship between California rainfall and ENSO events, *J. Climate*, *2*(11), 1258–1269, doi:10.1175/1520-0442.
Spracklen, D. V., L. J. Mickley, J. A. Logan, R. C. Hudman, R. Yevich, M. D. Flannigan, and A. L. Westerling (2009), Impacts of climate change from 2000 to 2050 on wildfire activity and carbonaceous aerosol concentrations in the western United States, *J. Geophys. Res.*, *114*, D20301, doi:10.1029/2008jd010966.
Sun, L. L., X. Y. Zhou, S. Mahalingam, and D. R. Weise (2006), Comparison of burning characteristics of live and dead chaparral fuels, *Combust. Flame*, *144*(1–2), 349–359, doi:10.1016/j.combustflame.2005.08.008.
Swetnam, T. W., and J. L. Betancourt (1990), Fire–Southern Oscillation relations in the Southwestern United States, *Science*, *249*(4972), 1017–1020, doi:10.1126/science.249.4972.1017.
Swetnam, T. W., and J. L. Betancourt (1998), Mesoscale disturbance and ecological response to decadal climatic variability in the American Southwest, *J. Climate*, *11*, 3128–3147, doi:10.1175/1520-0442.
Syphard, A. D., V. C. Radeloff, J. E. Keeley, T. J. Hawbaker, M. K. Clayton, S. I. Stewart, and R. B. Hammer (2007), Human influence on California fire regimes, *Ecol. Appl.*, *17*(5), 1388–1402, doi:10.1890/06-1128.1.
Uppala, S. M., et al. (2005), The ERA-40 re-analysis, *Q. J. Roy. Meteor. Soc.*, *131*(612), 2961–3012, doi:10.1256/qj.04.176.
van der Werf, G. R., J. T. Randerson, L. Giglio, N. Gobron, and A. J. Dolman (2008), Climate controls on the variability of fires in the tropics and subtropics, *Global Biogeochem. Cycles*, *22*, doi:10.1029/2007gb003122.
Viney, N. R. (1991), A review of fine fuel moisture modelling, *Int. J. Wildland Fire*, *1*(4), 215–234, doi:10.1071/WF9910215.

©2014. American Geophysical Union. All Rights Reserved.

Westerling, A. L., H. G. Hidalgo, D. R. Cayan, and T. W. Swetnam (2006), Warming and earlier spring increase western US forest wildfire activity, *Science*, *313*(5789), 940–943, doi:10.1126/science.1128834.

Westerling, A. L., A. Gershunov, T. J. Brown, D. R. Cayan, and M. D. Dettinger (2003), Climate and wildfire in the western United States, *Bull. Am. Meteorol. Soc.*, *84*(5), 595–604, doi:10.1175/BAMS-84-5-595.

Westerling, A. L., D. R. Cayan, T. J. Brown, B. L. Hall, and L. G. Riddle (2004), Climate, Santa Ana winds and autumn wildfires in southern California, *Eos Trans. AGU*, *85*(31), 289–296, doi:10.1029/2004EO310001.

Westerling, A. L., B. P. Bryant, H. K. Preisler, T. P. Holmes, H. G. Hidalgo, T. Das, and S. R. Shrestha (2011), Climate change and growth scenarios for California wildfire, *Clim. Change*, *109*(1), 445–463, doi:10.1007/S10584-011-0329-9.

©2014. American Geophysical Union. All Rights Reserved.